Electronic Supplementary Material (ESI) for Inorganic Chemistry Frontiers.

Supporting Information for

Highly efficient electrochemical ammonia synthesis using superhydrophobic nanoporous silver

Yating Qi[a], Ming Yang[a], Tian-En Zhao[a], Guorui Tang[a], Hongming He[a], Hongming Sun[a], Yijie Yang*[a], Cheng-Peng Li*[a]

[a]*College of Chemistry, Tianjin Key Laboratory of Structure and Performance for Functional Molecules, Tianjin Normal University, 300387 Tianjin, China*

*Corresponding authors:

E-mails: hxxyyyj@tjnu.edu.cn; hxxylcp@mail.tjnu.edu.cn

Calculation of ammonia yield rate and Faradaic efficiency

The Faradaic efficiency is calculated on the basis of the amount of electric charge used for synthesizing ammonia, which is divided by the total charge passed through the electrodes during the whole electrolysis (Faradaic efficiency =3F x n_{NH3}/Q). F is the Faraday constant; n_{NH3} is the ammonia amount produced in ENRR test and measured with indophenol method; and Q is the total quantity of applied electricity during the ENRR process. The ammonia yield rate is calculated based on the equation (v_{NH3} = n_{NH3}/(t x A_{cat})), where t is the ENRR time, and A_{cat} is the loading area of catalyst.

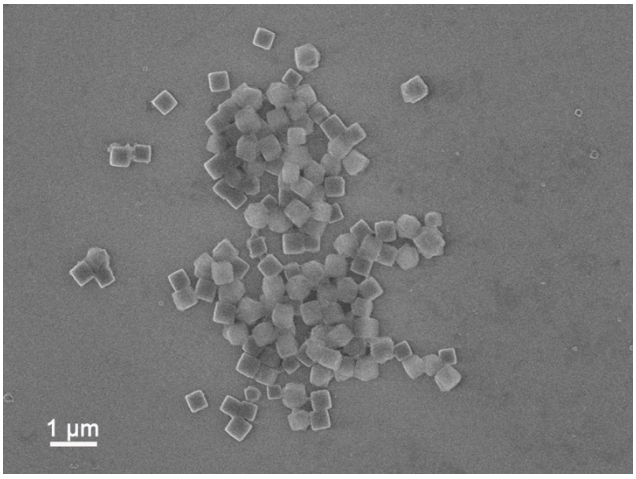

Figure S1. Scanning electron microscope (SEM) characterization of AgCl nanocubes.

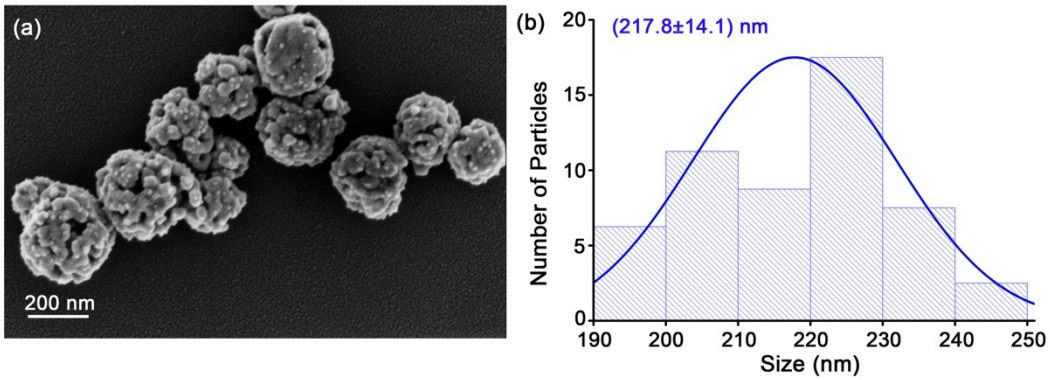

Figure S2. (a) SEM characterization of NPS and (b) the corresponding size distribution diagram.

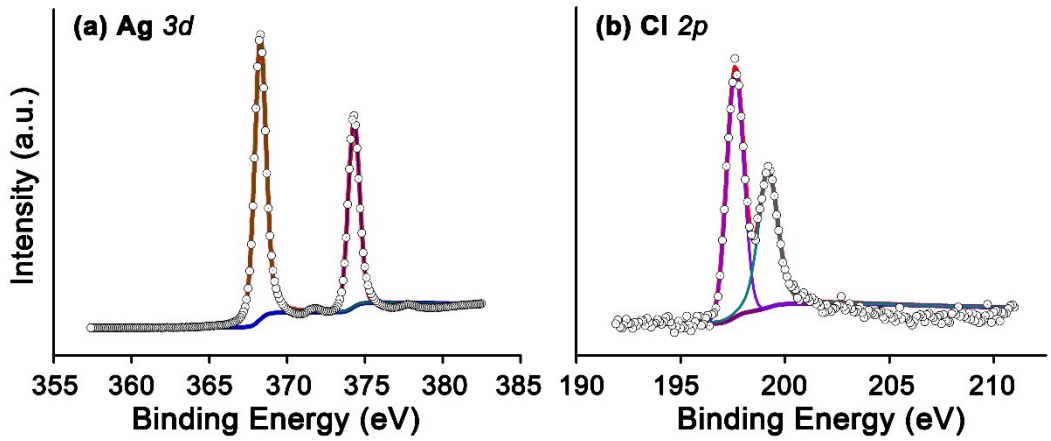

Figure S3. XPS spectrum at (a) Ag 3d, (b) Cl 2p

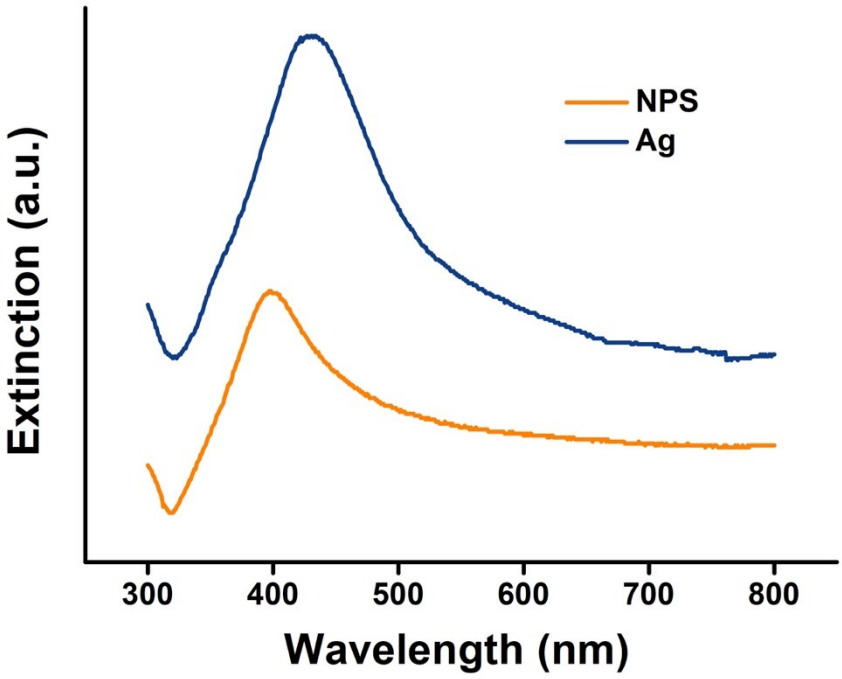

Figure S4. UV-vis spectra of NPS and solid Ag nanoparticles.

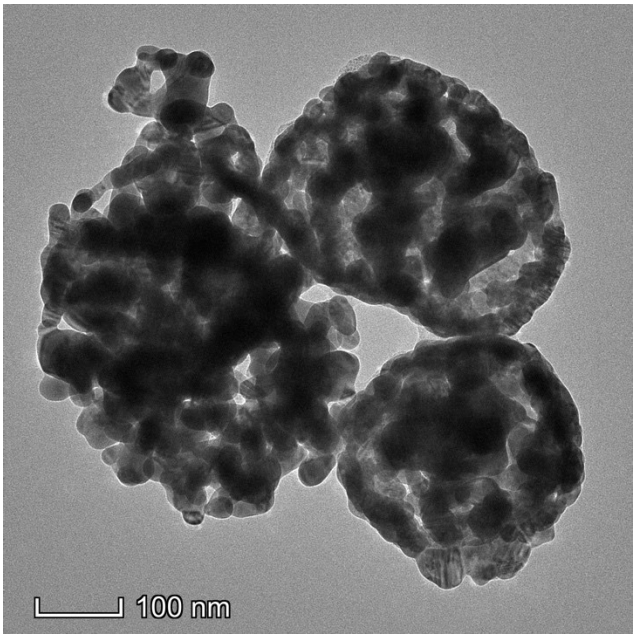

Figure S5. TEM image of SHNPS structures.

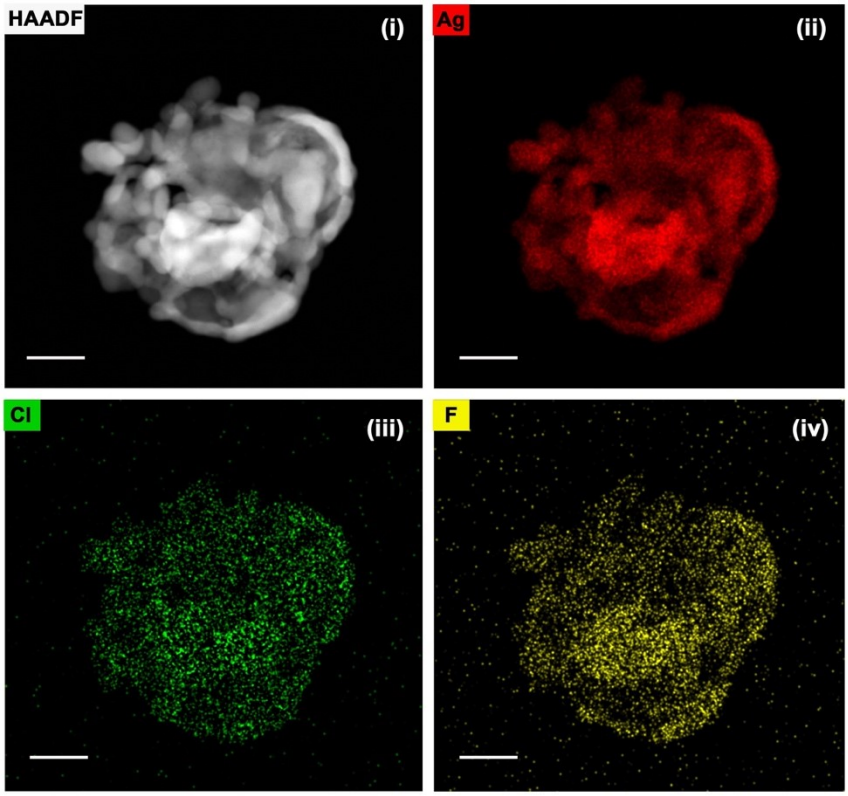

Figure S6. (i) HAADF-TEM image of SHNPS structures and the corresponding EDS elemental mapping indicating (ii) Ag, (iii) Cl, and (iv) F elemental distribution. Scale bar, 100 nm.

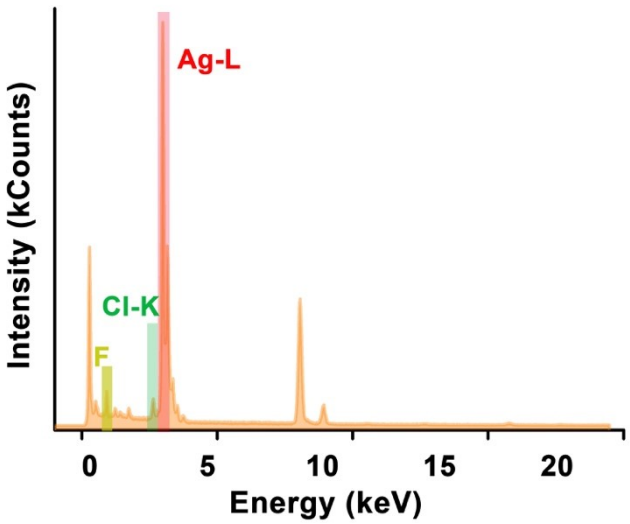

Figure S7. EDS elemental spectra showing peaks at F, Cl-K and Ag-L.

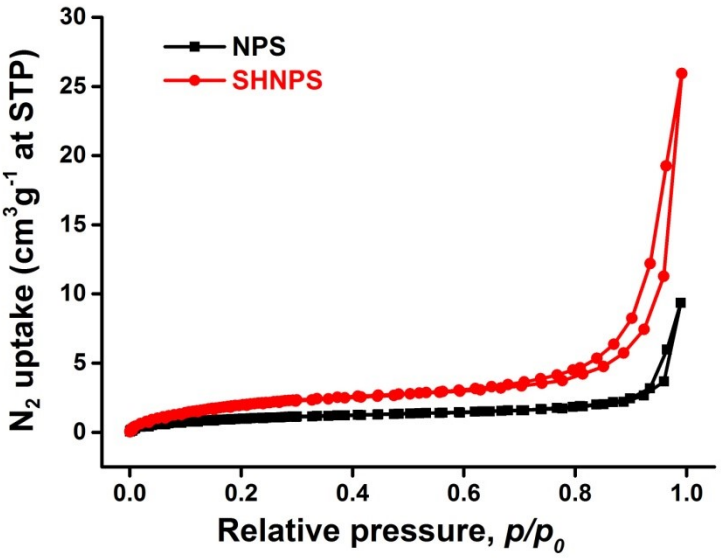

Figure S8. BET characterization of NPS and SHNPS

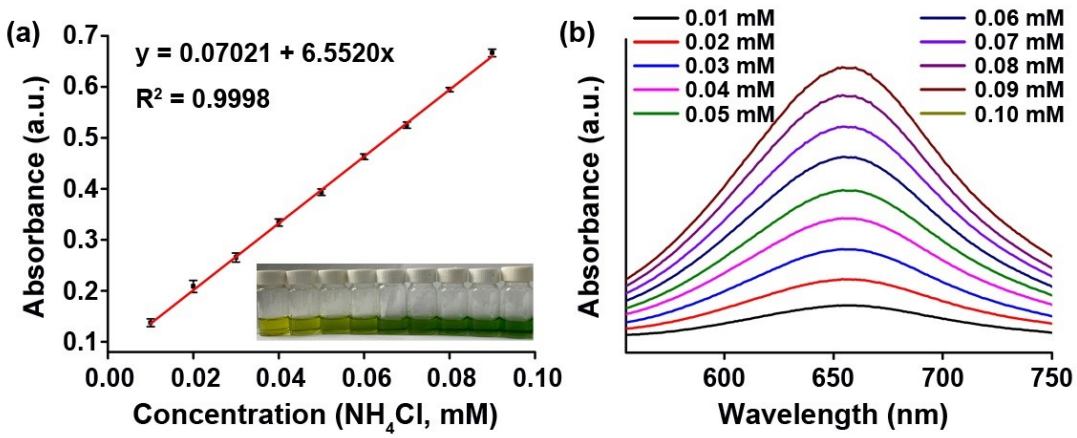

Figure S9. (a) Calibration curve and (b) UV-vis spectra of ammonia assay for various NH_4Cl concentration.

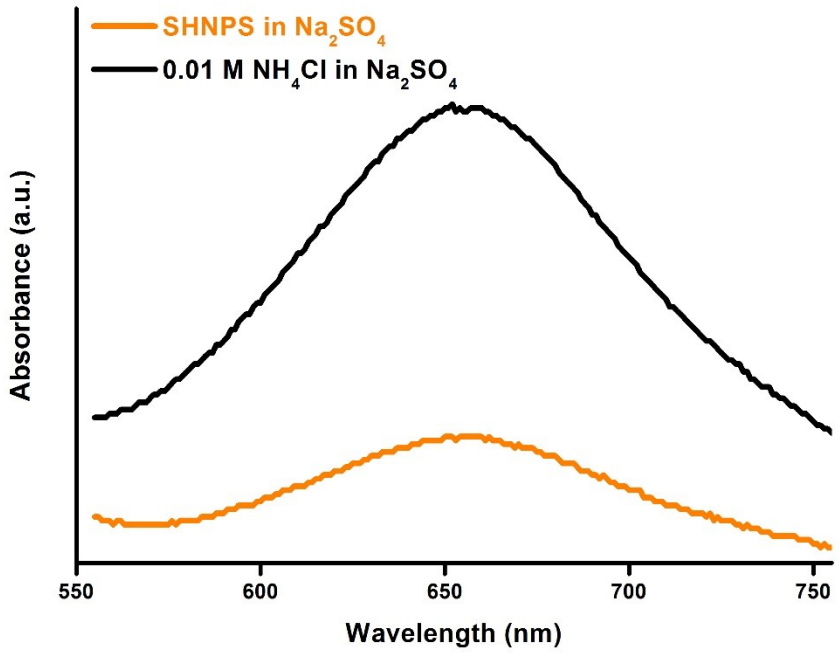

Figure S10. UV-vis spectra of SHNPS in the Na_2SO_4 aqueous solution using the same amount of SHNPS for ENRR tests.

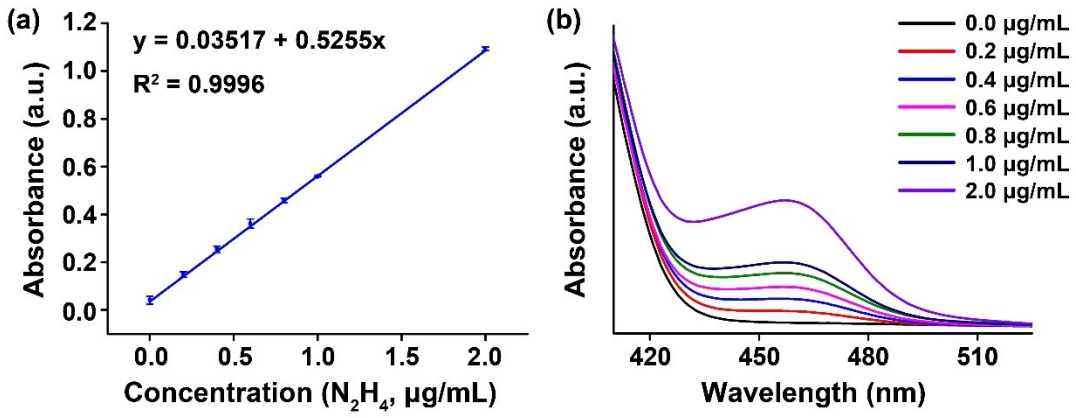

Figure S11. (a) Calibration curve and (b) UV-vis spectra of hydrazine as a reference for ENRR by-product determination.

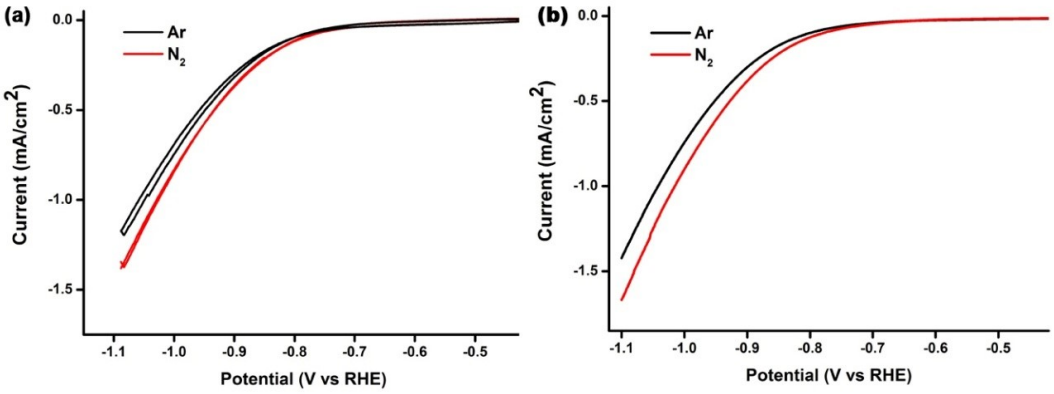

Figure S12. (a) CV and (b) LSV curves of SHNPS in the Ar- and N_2- saturated electrolyte.

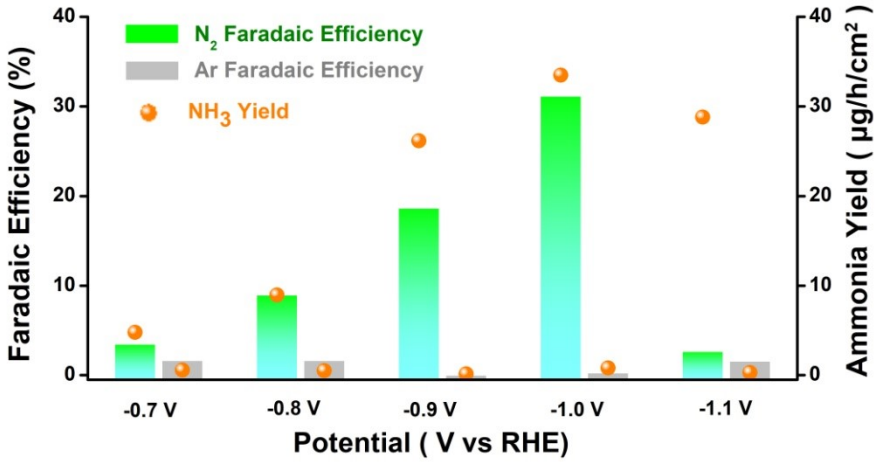

Figure S13. The comparison on ammonia yield rate and corresponding Faradaic efficiency in N_2 and Ar-saturated environment using SHNPS catalyst under various potentials.

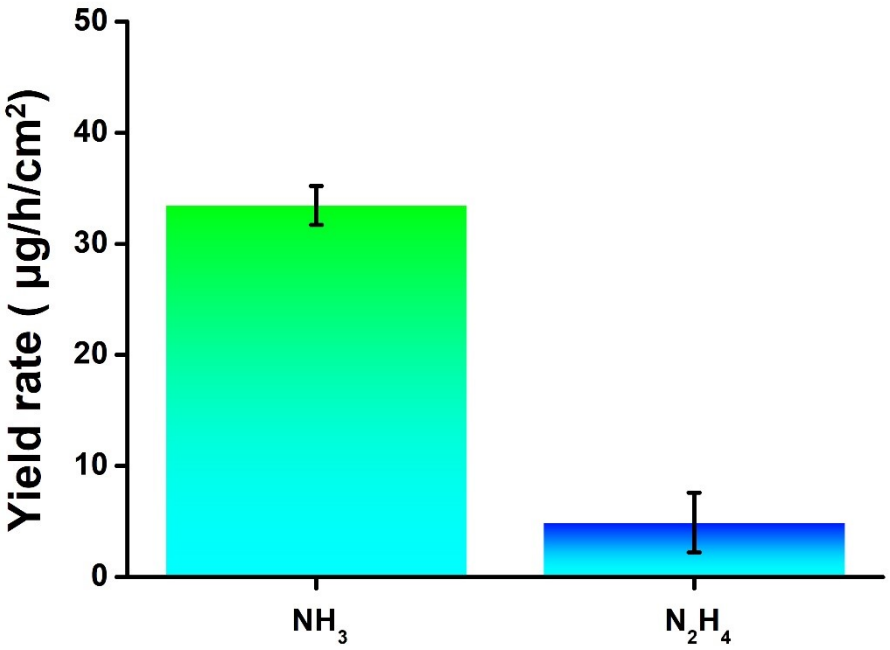

Figure S14. The yield of by-product of ENRR.

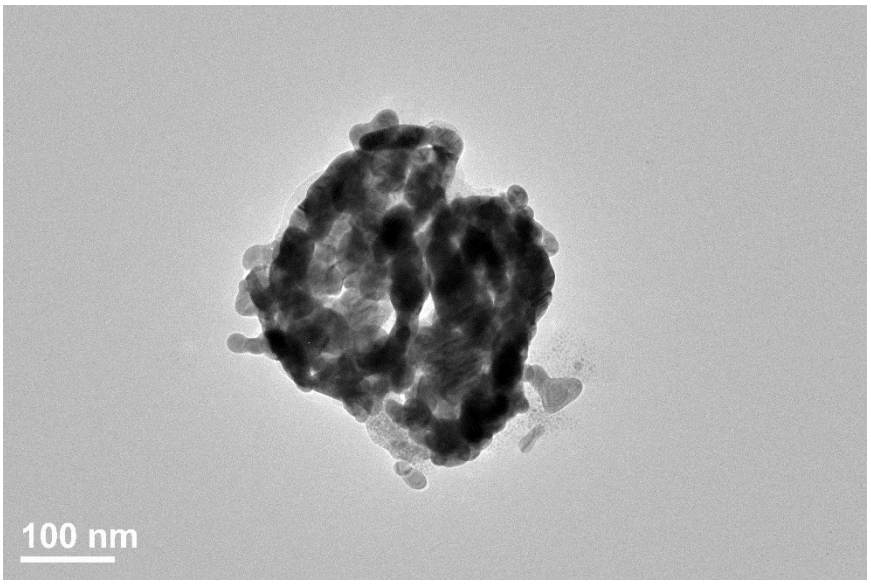

Figure S15. TEM image of SHNPS after catalyzing ENRR.

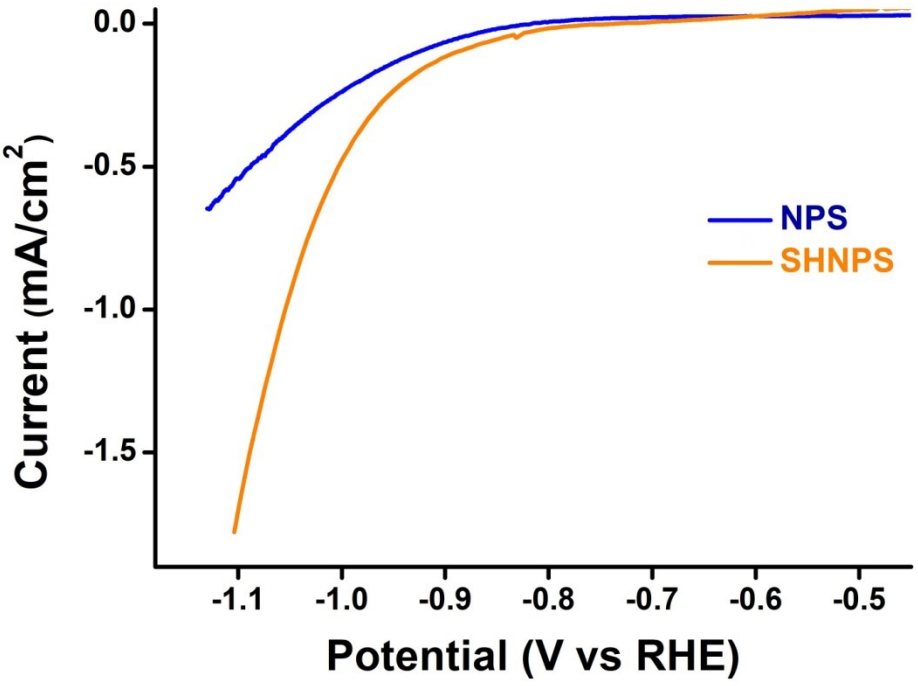

Figure S16. LSV curves of NPS and SHNPS in N_2-bubbling electrolyte.

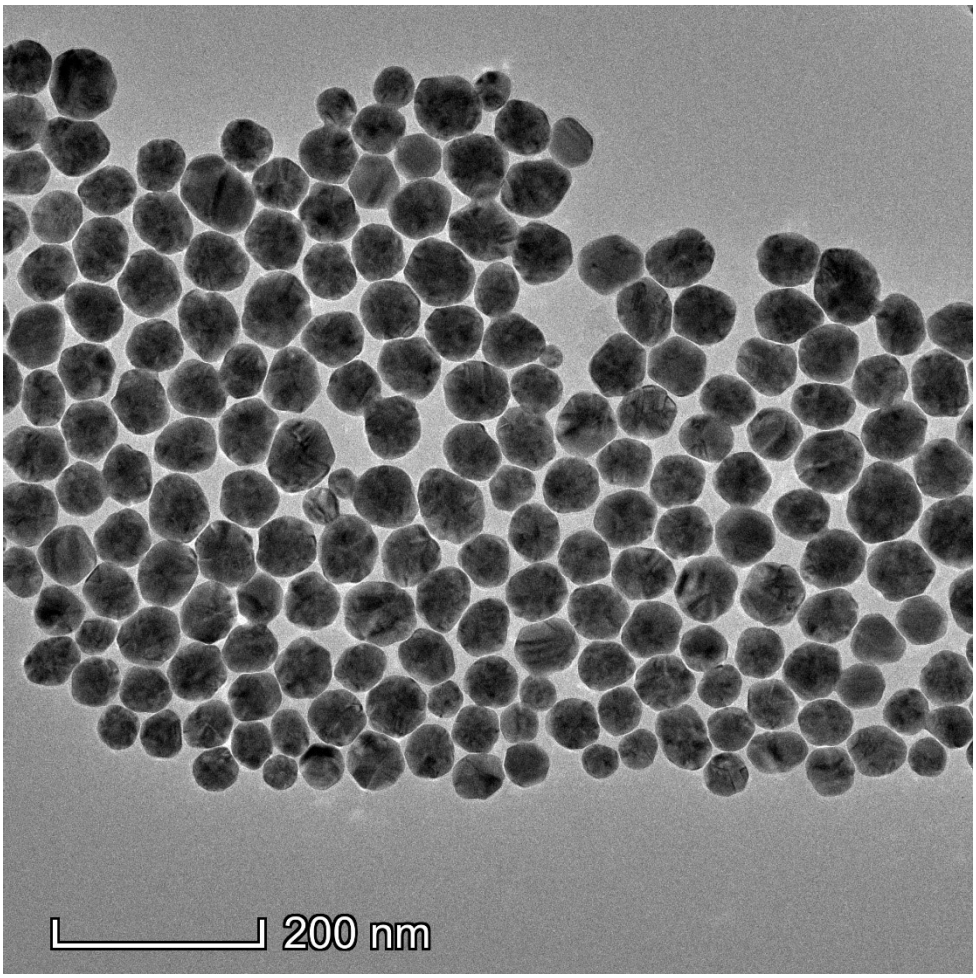

Figure S17. TEM characterization of solid Ag nanoparticles.

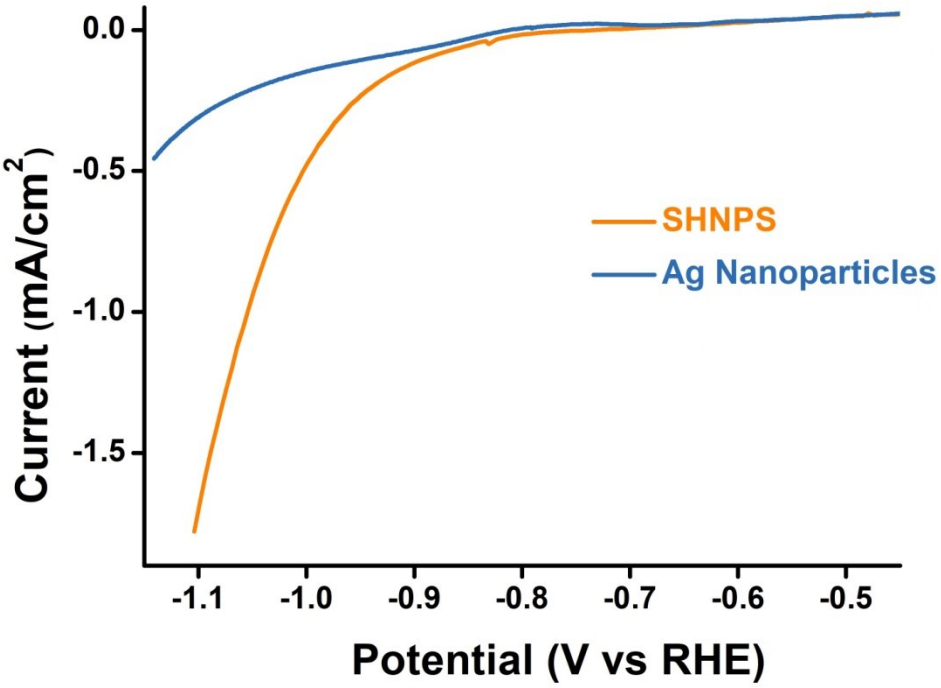

Figure S18. The comparison of LSV curves for SHNPS and solid Ag nanoparticles.

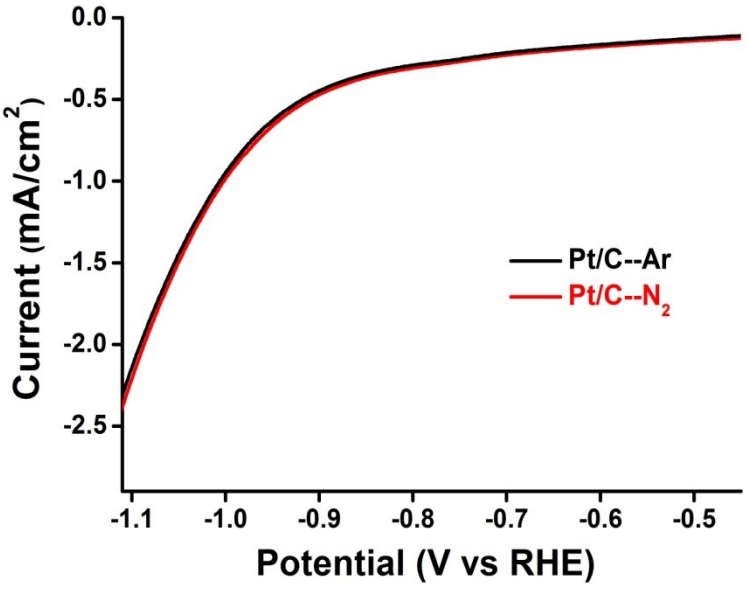

Figure S19. LSV tests of commercial Pt/C catalyst in Ar- and N_2- saturated electrolytes.

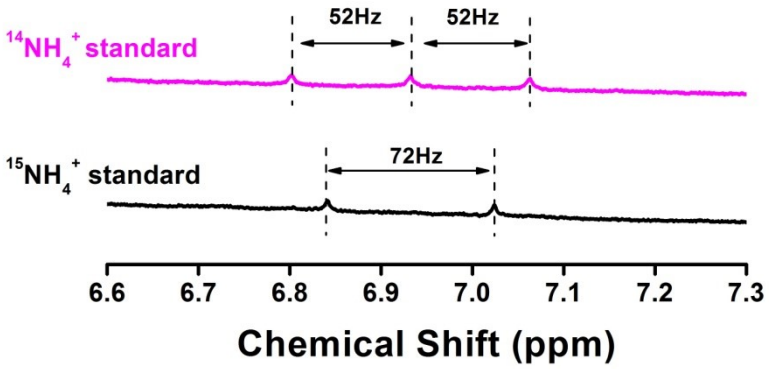

Figure S20. ^{1}H NMR spectra of the standard $^{14}NH_4Cl$ and $^{15}NH_4Cl$.